Comparative Study of Hybrid Powertrain Architectures from a Fuel Economy Perspective

Boli Chen, Xuefang Li, Simos A. Evangelou
Department of Electrical and Electronic Engineering
Imperial College London, UK

E-mail: boli.chen10@imperial.ac.uk

Topics/Powertrain Control and Energy Management Control

May 15, 2018

Depending on the structure of powertrain components, modern hybrid electric vehicles (HEVs) are usually categorized into different types, which influence the design and performance of energy management control strategies. This paper investigates the impact of non-plug-in HEV powertrain architectures on the fuel economy, where Dynamic Programming is used to find the optimal power split between the powertrain energy sources. The series and three parallel architectures that include through-the-road, pre- and post-transmission parallel, all with properly sized powertrain components, are compared. Three human-driver speed profiles collected respectively from urban, rural, and highway driving conditions are employed for the assessment. The comparative results demonstrate the energy saving potential of different types of HEVs and provide further insight into the practical choice of the hybrid powertrain architectures.

1 INTRODUCTION

Vehicle electrification plays a critical role in reducing CO_2 and NOx emissions. Depending on the degrees of electrification, there exist two types of electric vehicles: hybrid electric (HEV) and battery electric (BEV). Compared to the BEV where the battery is the only energy source, hybrid electric vehicles (HEV) is powered by two energy sources: the engine and the battery. As such, HEVs offer an environmental friendly solution, which has longer range than BEVs and improved fuel economy than conventional vehicles. There are several architectures in which the hybrid energy sources and other powertrain components are arranged, such as series, parallel and split-power architectures, with possible further subcategories in each case.

A series HEV is sometimes referred to as a range-extended electric vehicle, such as the BMW i3 range extender and the Nissan Note e-power. The series powertrain architecture represents the simplest structure as all the driving power is delivered to the wheels by the electric motor, which receives electric power from either the engine or the battery. Although a very large motor is usually required, the engine greatly benefits from this architecture, since it is mechanically decoupled from the wheels, therefore allowed to be operated at its optimal point persistently. This fact makes series structure favorable during urban driving. In the context of a parallel HEV, both the engine and the battery separately drive the wheels. The direct connection between the engine and the wheels avoids the double energy conversion losses associated with the series architecture, and it thus offers enhanced fuel efficiency for highway driving. In addition, the parallel architecture is often sub-categorized into pre-transmission, post-transmission, and through-the-road (TTR), wherein the pre- and post-transmission are distinguished by the arrangement of the gearbox. Vehicles of these types include the Honda Insight and Civic. On the other hand, the TTR represents an alternative with low mechanical complexity as the battery and engine act on different axles (thus the engine branch amounts to a conventional drivetrain) instead of driving the same axle, which requires additional components for coupling. Such a configuration makes TTR a very suitable solution for the hybridization of conventional vehicles. The BMW i8 and the Peugeot 3008 are examples of TTR HEVs in the market. The split-power architecture (which is usually referred to as series-parallel) essentially combines the series and the parallel structures in one framework, which may allow the powertrain to be switched within different modes based on road types (e.g., GM Volt, Toyota Prius). As such, a split-power HEV is possible to deliver improved fuel economy than series and parallel which may excel only in a particular road type. However, the powertrain complexity and the cost may be significantly increased [11, 16]. The operation scheme of the split-power HEV makes it important to understand the individual behavior of the series and parallel architectures.

The investigation of the impact of powertrain architectures on the fuel economy requires an energy management strategy (EMS) to be uniformly deployed for all structures. Thus, for given vehicle loads the power-split pattern between multiple energy sources is equally optimized. A large number of EMS, from rule-based to optimization-based, have been proposed in the literature for fuel consumption minimization [18, 5, 3, 6, 14, 9, 7]. The rule-based methods are usually referred to as heuristic strategies, which are based on simple control policies, such as the thermostat approach [16]. Although some recently proposed heuristic EMS can highly resemble the optimization solutions, global optimality is not guaranteed and the specific rules are powertrain architecture dependent [16, 17, 13, 1]. Therefore, it is not suitable to use rule-based strategies for this study. On the other hand, the energy management problem can be formulated as an optimal control problem (OCP), where the vehicle powertrain model and the operational constraints are included as differential and inequality constraints. As such, the optimization approaches are not limited to a particular HEV configuration and can be easily applied to any type of HEV. There exist a variety of techniques in the literature for solving this OCP, including dynamic programming (DP), nonlinear programming and Pontryagin's minimum principle (PMP), which produce more optimal solutions than those of the heuristic strategies [2, 8, 15]. This fact turns out to be useful for the study in this paper.

In this paper, the influences of non-plug-in HEV powertrain configurations on the optimal power split and the resulting fuel economy are studied. Four commonly used architectures, including series, and the three parallel configurations, post-transmission, pre-transmission, and the TTR, are considered and modeled in this work. As the overall energy efficiency is strongly influenced by the sizes of the powertrain components (which affects the vehicle mass, capability of energy regeneration, etc.), the internal combustion engine (ICE), battery and electric machine (EM) of all HEVs have been scaled on a basis of identical powertrain cost, for a fair comparison. The energy management control tasks are formulated as OCPs, which are then solved by DP [4] for the guarantee of a global optimum in fuel consumption. The drive missions are specified in terms of real-world driving speed profiles, which tend to produce more realistic test environments than the widely used standard test cycles. Different driving conditions have been tested to demonstrate the potential benefits of each HEV architecture and to enable the appropriate selection of hybrid architectures based on the drivers needs.

The remainder of the paper is structured as follows. Section 2 introduces the hybrid powertrain architectures to be studied in this paper, while the tested driving cycles are demonstrated in Section 3. In Section 4 an OCP is formulated to solve the energy management problems for different powertrain structures. Simulation results and discussion are presented in Section 5. Finally, concluding remarks are given in Section 6.

2 HYBRID ELECTRIC VEHICLE MODELING

In a series HEV, the electric motor is the only means to deliver propulsion power to the vehicle wheels. Such scheme allows the ICE to be mechanically decoupled from the wheels to provide great flexibility in the engine operation. However, an additional electric generator is required, and the traction motor tends to be large in this case, leading to supplementary weight, cost and another stage of energy conversion. In a parallel HEV, the ICE is directly connected to the wheels via the gearbox, and it thus cancels the associated energy conversion losses as presented in the series architecture. There are multiple ways for the motor to drive the wheels in parallel with the ICE. As it can be seen in Fig. 1, the battery branch (via the motor) is coupled to the ICE branch after the transmission system in the post-transmission fashion, whereby the motor speed is directly coupled to the vehicle speed and provides power without suffering from additional transmission losses. However, a large motor is usually required as it is expected to be operated at a very high torque when the vehicle is driven at a low speed. Conversely, in the pre-transmission system, both the motor and ICE are located before the transmission system, where the ICE power and the motor power are merged at the same operating speed. The mutual gearbox allows the motor to be downsized by constantly operating it at high speed and low torque. The TTR offers a four-wheel driving solution by utilizing the ICE and the motor separately on the front and the rear axles. Although the battery and the ICE act on different axles, the battery in this case can still be recharged by the ICE though the road. Since the axle driven by the ICE is identical to that of a conventional powertrain, it is very convenient to turn a conventional vehicle into a hybrid subject to the TTR configuration.

The split-power architecture has recently become a very popular solution in the market as it is allowed to take advantage of both series and parallel HEVs. These benefits come at the expense of additional electric machines and power split devices, typically a planetary gear set. Consequently, the main drawback of the split-power structure is the significantly increased mechanical complexity and cost. The comparative study perfomed in this paper (of the series and parallel architectures only) also has important practical implications for split-power architectures, which allow multi-mode operation formed by the single series and the single parallel schemes shown in Fig. 1.

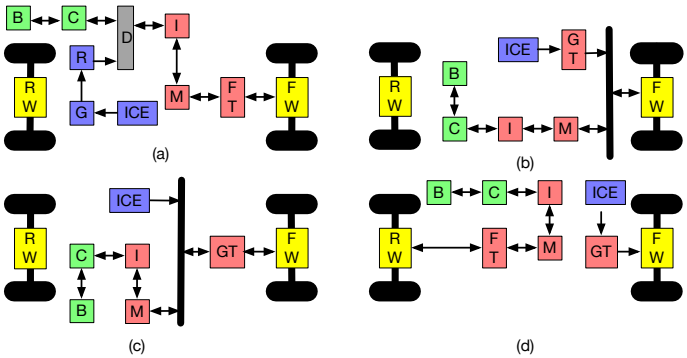

Figure 1: HEV powertrain architectures. (a) Series; (b) post-transmission; (c) pre- transmission; (d) TTR. B: battery, C: dc/dc converter, G: generator, M: motor, I: DC/AC inverter, GT: gearbox, FT: fixed transmission; D: DC-link, R: AC/DC inverter; FW: front axle, RW: rear axle.

It is clear that there is a fundamental trade-off between computational cost and accuracy in the HEV powertrain modeling. The individual powertrain components are first modeled following the HEV model introduced in [10], with the aim to capture the essential physics without involving significant model complexity. As such, the overall powertrain models of the studied HEVs are appropriate for DP in terms of dynamic order. More specifically, the ICE and the electric machine (EM) are simply modeled as steady state efficiency maps with respect to the angular speed and torque as the mechanical inertia of the powertrain branch is much smaller than the overall vehicle inertia. The fuel consumption m_f in each case is evaluated by the associated fuel consumption maps, for example, Fig. 2 shows the fuel mass rate of an ICE with respect to its torque and speed. When a different ICE is utilized, the fuel consumption map needs to be re-scaled based on the size of the engine. Typically, the series architecture

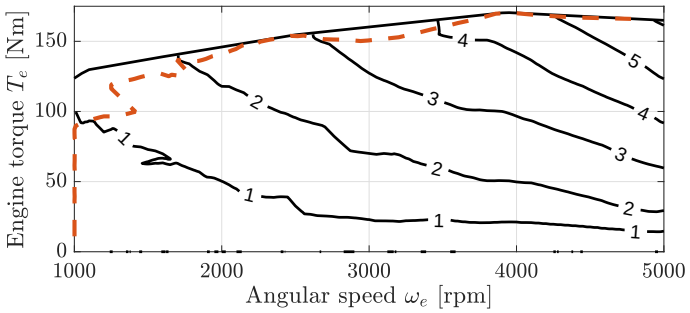

Figure 2: Fuel mass rate [g/s] of the engine branch with torque and speed operating points. The ICE produces a peak power of 86.38kW at 5000 rpm, a peak torque of 170 Nm at 3950 rpm. The torque-speed operating points for maximum engine branch efficiency at different output power values are shown by a dashed curve, which can be followed in a series HEV.

allows the ICE to be optimally operated independently of the vehicle speed, whereby the engine is assumed to be operated along a locus of the most efficient torque-speed operating points for all possible engine power, as shown by the dashed curve in Fig. 2.

The battery is modeled as a pure integrator with purely ohmic impedance. Furthermore, instead of using a nonlinear mapping between state-of-charge (SOC) and the open circuit voltage (denoted by V_{oc}), V_{oc} is reasonably approximated by a constant voltage of 300 V, which is compatible with the usual aim of a charge sustained battery management, by which the battery state-of-charge (SOC) is narrowly constrained. Hence, the SOC is the only state variable, which is governed by:

$$\frac{d}{dt}\text{SOC} = -\frac{i_b}{Q_{\max}}. \tag{1}$$

where $Q_{\max}$ is the battery capacity, i_b denotes the battery current, assumed positive during the discharge phase. The current

of the internal resistance electrical model can be solved with respect to V_{oc}, the battery output power P_b and internal resistance R_b, as follows:

$$i_b = \frac{V_{oc} - \sqrt{V_{oc}^2 - 4P_bR_b}}{2R_b}. \tag{2}$$

Then, the battery model is described by

$$\frac{d}{dt}\text{SOC} = \frac{V_{oc} - \sqrt{V_{oc}^2 - 4P_bR_b}}{2R_bQ_{\max}}. \tag{3}$$

The power losses of power inverters and transmission systems, including the fixed transmission and gearbox have been considered and modeled as constant efficiency terms. Mechanical brakes are applied to both front and rear wheels, whereas the regenerative brakes are only performed at the axle connected to the motor. In this work, it is assumed that the brake distribution is always fixed and 2/3 of braking power can be regenerated, while the rest is met by the mechanical brakes.

By assembling the models of individual components, the powertrain systems of the studied architectures are obtained. As it can be noticed, the battery SOC is the only dynamic state, which evolves according to (3). Such one state systems allow DP to be efficiently implemented in all cases.

Since the fuel economy is influenced by the size of the energy sources that is specified in terms of power and weight, the components must be properly scaled for fair comparisons. In this framework, we introduce a metric of component cost that is the sum of the costs for the ICE unit (with either gearbox or generator embedded depending on the architecture), EM and battery on a vehicle, whereas the remaining costs of the powertrain components are omitted for simplicity as those costs are almost independent of the size (for example electronic converters). In order to reduce the number of sizing variables, the battery size is fixed to 1.5 kWh, with the power operated within $[-15, 30]$ kW (i.e., c-rate limits are 20 C and 10 C for discharging and charging respectively) for all configurations and the costs and masses of the generator and gearbox are assumed to be equivalent. Also, in the parallel architectures the EM is matched to the battery in terms of peak power and the ICE has a fixed size. Then the ICE and EM in the series architecture are scaled, such that all the architectures have the same cost. The relationships between the costs and masses of the ICE, the EM and the battery with respect to their sizes are assumed linear, provided the components are scaled within $[50\%, 200\%]$ of the baseline [12]. The baseline size of the ICE and EM in the work are 65 kW, 97.5 kg and 35 kW, 48 kg, respectively. The cost, c, and mass, m, are computed by

$$c_i = c_{i,0} + c_{i,1}s, \tag{4}$$

$$m_i = m_{i,1}s \tag{5}$$

where $i \in \{\text{EM, ICE}\}$, s is the scale factor, e.g., $s = 2$ if a 130 kW ICE is utilized, $c_{EM,0} = 1750$,$c_{EM,1} = 875$, $c_{ICE,0} = 575$, $c_{ICE,1} = 667$,$m_{EM,1} = 48$ kg and $m_{ICE,1} = 97.5$ kg [12]. Let the mass of the vehicle without ICE and EM equal to 1278 kg, identical for all cases, then the gross vehicle masses are determined by

$$m = 1278 + m_{EM} + m_{ICE} \tag{6}$$

Finally, the sizes of the ICE and the EM for all parallel HEVs are 120 kW and 30 kW respectively whereas the ICE is 35 kW and the EM is 65 kW for the series, yielding the same cost and $m = 1500$ kg for parallels, $m = 1420$ kg for the series. As it can be seen, the series powertrain is more costly than the parallels to produce the same peak power, as a larger motor is required. Consequently, the series powertrain tends to be bulky, and mainly utilized on heavy and large vehicles in practice.

3 DRIVING CYCLES

The driving cycle defines the speed profile that needs to be followed by the vehicle, it thus heavily influences the operation of the EMS and the overall fuel economy. For a better reflection of the real-world driving conditions (e.g., traffic lights, grades), including human drivers' inclination (e.g., usually apply higher acceleration and deceleration than standard cycles), experimental driving speed profiles are utilized. The time history data are recorded by a recently developed data acquisition device [19] respectively for urban, rural and motorway driving to perform a comprehensive assessment. The speed profiles are shown in Fig. 3, with some of their particular features specified in Table 1.

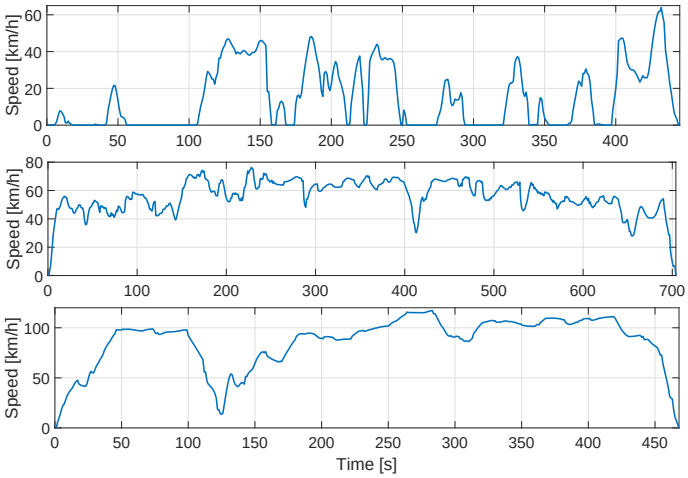

Figure 3: Real-world speed profiles. Top: urban; Middle: rural; Bottom: motorway.

Table 1: Characteristics of tested speed profiles

	Urban	Rural	Motorway
Duration [s]	445	704	468
Distance [km]	1.84	10.95	11.21
Average Speed [km/h]	14.8	56	86.3
Max speed [km/h]	63.9	76.3	117.2
Max acceleration [m/s^2]	5.55	2.34	2.33
Max deceleration [m/s^2]	-6.96	-3.64	-3.44
Avg. load for Parallel [kW]	1.65	4.40	11.55
Avg. load for Series [kW]	1.60	4.39	11.53

For a given driving cycle, the power demand at the driving wheels P_{drive} can be uniquely determined by

$$P_{drive} = (m\,a + \gamma_t m\,g + \gamma_d v^2)\,v \tag{7}$$

where m is the vehicle mass, v is the vehicle speed and a is the vehicle acceleration, $\gamma_t = 0.01$ and $\gamma_d = 0.47$ are the tire resistance coefficient and the aerodynamics drag coefficient, respectively (the average values of P_{drive} in different driving scenarios are provided in Table 1). Consequently, P_{drive} is used as the input of the energy management control system instead of the driving cycles, whereby the dynamics of the vehicle longitudinal model can be removed. P_{drive} is met throughout the mission by the powers received from the two energy sources.

Moreover, the series architecture allows further reduction of the control system complexity since it is possible to refer the power at the wheels, P_{drive}, to the power demand P_{PL} at the DC-link, as follows:

$$\begin{cases} P_{PL} = \dfrac{P_{drive}}{\eta_{PL}}, \forall\, P_{drive} \geq 0, \\ P_{PL} = (P_{drive} - P_h)\eta_{PL}, \forall\, P_{drive} < 0. \end{cases} \tag{8}$$

where P_h is the mechanical braking power directly applied to the wheels, and η_{PL} is the combined efficiency of the inverter,

motor and the transmission that only depends on the conditions imposed by the driving cycle, but not the energy management. As such, the powertrain model for the energy management optimization of the series HEV can be simplified to the engine and battery branches only with P_{PL} the reference input that is satisfied throughout the simulation.

4 OPTIMAL CONTROL FORMULATION

The power-split between hybrid energy sources throughout the whole mission is addressed by DP in this study. In order to implement DP, the following OCP is formulated:

$$\min_{\mathbf{u}} \quad m_f(T)\,, \tag{9a}$$

$$\text{subject to:} \quad \dot{\mathbf{x}} = \mathbf{f}(\mathbf{x}, \mathbf{u}, t)\,, \tag{9b}$$

$$\psi(\mathbf{x}, \mathbf{u}, t) \leq \mathbf{0}\,, \tag{9c}$$

$$\mathbf{b}(\mathbf{x}(0), \mathbf{x}(T)) = \mathbf{0} \tag{9d}$$

where T is the time duration of the simulation and amounts to the length of the driving cycle, as reported in Table 1. Equation (9b) represents the dynamic model of the powertrain system, where $\mathbf{x} \triangleq$ SOC is the only state governed by (3). The control input $\mathbf{u}$ is formed by the engine and battery power, which together fulfill the requested power demand P_{drive} (or P_{PL} for series HEV). As it can be noticed, when $P_{drive} < 0$ (or $P_{PL} < 0$ for series HEV), only the battery is used for energy recovery, therefore the energy management control is essentially applied only to the phase when $P_{drive} \geq 0$ (or $P_{PL} \geq 0$ for series HEV). The inequality constants (9c) comprise

$$\text{SOC}_{\min} \leq \text{SOC} \leq \text{SOC}_{\max}\,, \tag{10}$$

$$0 \leq P_{ICE} \leq P_{ICE_{\max}}\,, \tag{11}$$

$$P_{b_{\min}} \leq P_b \leq P_{b_{\max}} \tag{12}$$

which are needed to keep the powertrain components operated inside their admissible range. As it can be noticed, $P_{ICE_{\max}}$, $P_{b_{\max}}$ and $P_{b_{\min}}$ represent the power limits of the engine and the battery, specified by the component sizes. SOC is limited within a narrow band $[\text{SOC}_{\min}, \text{SOC}_{\max}] = [50\%, 80\%]$. The boundary conditions (9d) define the initial and terminal conditions of the state variable: $\text{SOC}(0) = \text{SOC}(T) = 65\%$. Therefore, the possible equivalent fuel caused by the non-zero differences between the initial and terminal conditions of SOC is always canceled, and makes it possible to compare fuel economy of each architecture in terms of m_f alone.

5 SIMULATION RESULTS

In this paper the DP algorithm developed in [4] is implemented in the Matlab environment as the benchmarking energy management strategy. The formulated OCPs in the form of (9) are discretized by the Euler method with sampling period $T_s = 0.1\,\text{s}$, together with a reasonably large number of mesh grid points for the state and control variables to ensure a high level of accuracy.

The optimal power profiles of the battery and the engine with the concerned architectures are solved for the urban, the rural and the highway driving cycles, respectively. As the optimal operational rules are equally reflected in each driving scenario, only the power-split profiles for the urban driving cycle are shown, as an example, in Fig. 4.

It can be observed that the optimal operation of the series HEV never uses the engine to charge the battery, which is easily verified by the fact that the engine power never exceeds P_{PL}. Since the battery is only charged through the regenerative braking, the overall battery usage may be very limited, and the gain from the additional electric power source may be limited in the series HEV. Conversely, for the parallel HEVs, it is worthwhile to operate the engine at a higher power than the requested operating power for some P_{drive} values, whereby the engine is optimally operated and the extra energy is stored in the battery for future use. Such operation can be observed in Fig. 4, for example, around $t = 225$ and $t = 330\,\text{s}$ of the parallel cases. Furthermore, the optimal solutions of all the HEVs allow the hybrid powertrain to be operated in the battery-only mode when a low operating power is requested, typically, around $t = 40\,\text{s}$ of the parallel cases and around $t = 10\,\text{s}$ for the series case. It is worth pointing out that the optimal power-split profiles of the post-transmission and the TTR are very close to each other as the energy flow paths of both structures are essentially similar. However, the engine of the TTR HEV charges the battery through the road rather than through the mechanical coupling device.

The battery SOC profiles are shown in Fig. 5. As it can be seen, the SOC in each case is successfully constrained with the admissible range. It is verified that the battery usage of the series hybrid is very limited in all driving scenarios, and is always less than that of the parallel configurations where the optimal solution allows the battery to be charged by the engine, as mentioned previously.

Finally, the fuel economy results for these powertrain architectures are compared in Fig. 6. As it can be seen, the post-transmission parallel offers the best combined fuel economy. The pre-transmission architecture is very sensitive to the driving speed profile. The gearbox switching improves the motor efficiency during urban driving which contains significant speed variations because of intensive traffic. However, the benefit vanishes when the vehicle is driven on a motorway as the gear is barely changed. TTR is slightly less efficient than the post-transmission structure, but it saves cost from the exclusion of the torque coupling device. Series HEV consumes more fuel than the parallel HEVs, especially on the motorway since the engine is not directly connected to the wheels. The series HEV fuel economy is improved for urban driving, but it still lags the post-transmission by 6%.

6 CONCLUSIONS

The comparison between different hybrid powertrain architectures in terms of fuel economy is addressed in this paper. It is shown that the parallel architectures are more economical than the series, which is usually more expensive due to the need for a larger motor. Among the parallel structures, the post-transmission has the best overall energy efficiency, while the TTR is less efficient than the post-transmission but it offers great flexibility in turning a conventional vehicle into a hybrid. Pre-transmission HEV can be designed to be very efficient for certain driving scenarios whereas the performance in the other cases may be sacrificed.

REFERENCES

[1] Bernd M. Baumann et al. “Mechatronic Design and Control of Hybrid Electric Vehicles”. In: *IEEE Transactions on Mechatronics* 5.1 (2000), pp. 58–72.

[2] Boli Chen, Simos Evangelou, and Roberto Lot. “Impact of Optimally Controlled Continuously Variable Transmission on Fuel Economy of a Series Hybrid Electric Vehicle”. In: *European Control Conference*. Limassol, Cyprus, 2018.

[3] D. A. Crolla et al. “Controller design for hybrid vehicles – state of the art review”. In: *Vehicle Power and Propulsion Conference, 2008. VPPC ’08. IEEE*. Sept. 2008, pp. 1–6. DOI: 10.1109/VPPC.2008.4677808.

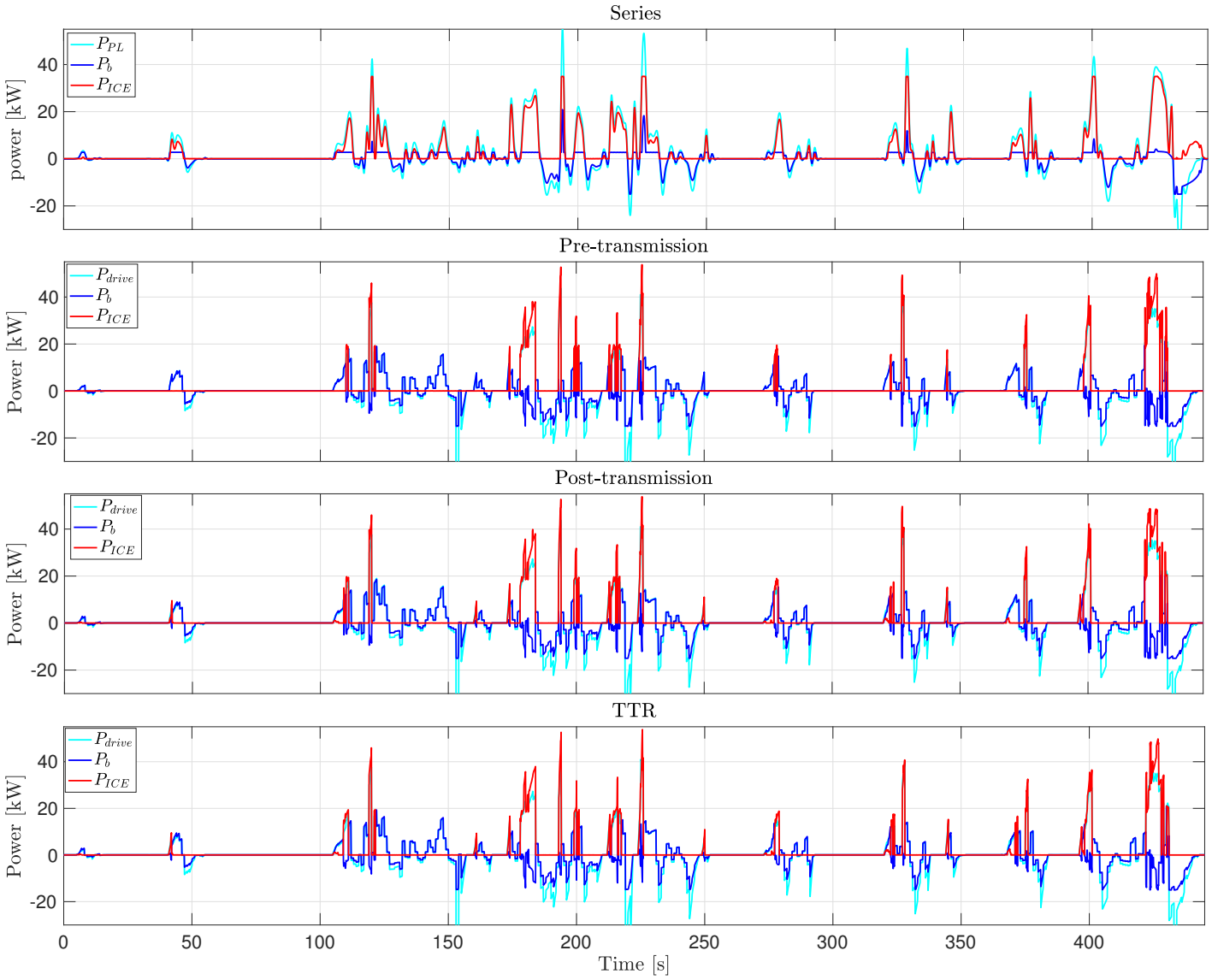

Figure 4: The optimal power profiles of different architectures when driving the urban speed profile.

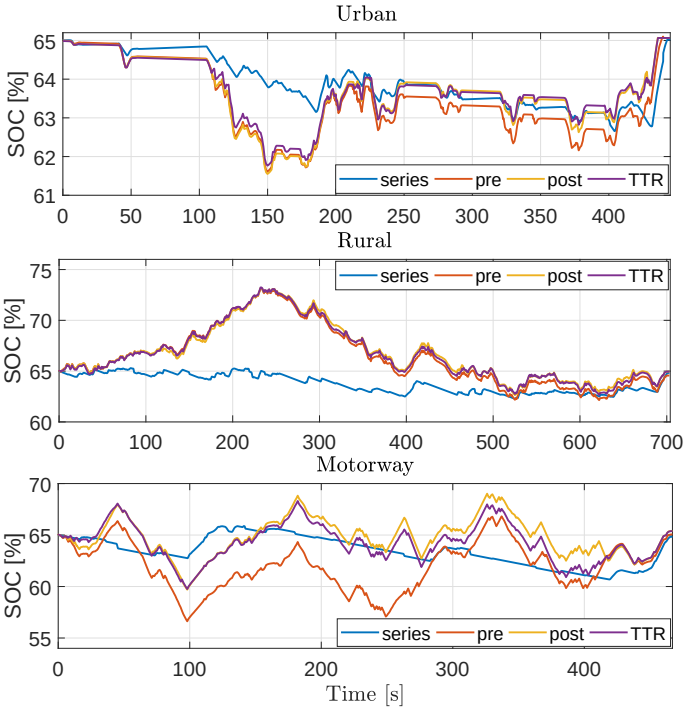

Figure 5: The optimal battery SOC profiles of different architectures in different scenarios.

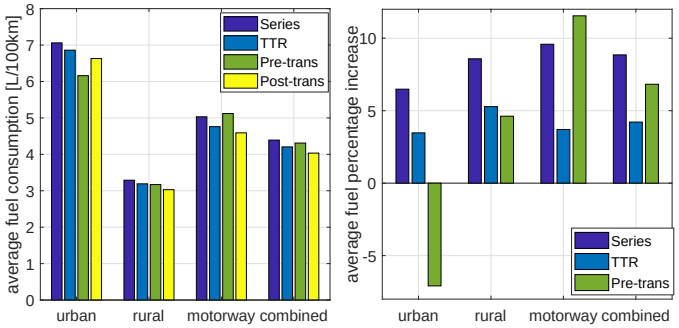

Figure 6: Left: Average fuel consumption in different scenarios; Right: Average fuel percentage increase on the basis of post-transmission solutions.

[4] Philipp Elbert, Soren Ebbesen, and Lino Guzzella. "Implementation of Dynamic Programming for n-Dimensional Optimal Control Problems With Final State Constraints". In: *IEEE Transactions on Control Systems Technology* 21.3 (2013), pp. 924–931.

[5] F. R. Salmasi. "Control strategies for hybrid electric vehicles: evolution, classification, comparison, and future trends". In: *IEEE Trans. Veh. Technol.* 56.5 (Sept. 2007), pp. 2393–2404.

[6] X. He, M. Parten, and T. Maxwell. "Energy Management Strategies for a Hybrid Electric Vehicle". In: *Proceedings*

of the 2005 IEEE Vehicle Power and Propulsion Conference. 2005, pp. 536–540.

[7] S. Kutter and B. Baker. "Predictive online control for hybrids: Resolving the conflict between global optimality, robustness and real-time capability". In: *Vehicle Power and Propulsion Conference (VPPC), 2010 IEEE*. Sept. 2010, pp. 1–7. DOI: 10.1109/VPPC.2010.5729231.

[8] L. Serrao, S. Onori, and G. Rizzoni. "ECMS as a realization of Pontryagin's minimum principle for HEV control". In: *American Control Conference, 2009. ACC '09.* June 2009, pp. 3964–3969. DOI: 10.1109/ACC.2009.5160628.

[9] L. V. Pérez and E. A. Pilotta. "Optimal power split in a hybrid electric vehicle using direct transcription of an optimal control problem". In: *Math. and Comput. in Simulation* 79.6 (Feb. 2009), pp. 1959–1970.

[10] Roberto Lot and Simos A. Evangelou. "Green Driving Optimization of a Series Hybrid Electric Vehicle". In: *52nd IEEE Conference on Decision and Control*. 2013, pp. 2200–2207.

[11] Jerome Meisel, Wassif Shabbir, and Simos Evangelou. "Evaluation of the Through-the-Road Architecture for Plug-In Hybrid Electric Vehicle Powertrains". In: *IEEE International Electric Vehicle Conference*. 2013.

[12] M. Pourabdollah et al. "Optimal Sizing of a Parallel PHEV Powertrain". In: *IEEE Transactions on Vehicular Technology* 62.6 (2013), pp. 2469–2480.

[13] N. Schouten, M. Salman, and N. Kheir. "Energy management strategies for parallel hybrid vehicles using fuzzy logic". In: *Control Engineering Practice* 11 (2003), pp. 171–177.

[14] A. Sciarretta, M. Back, and L. Guzzella. "Optimal control of parallel hybrid electric vehicles". In: *IEEE Transactions on Control Systems Technology* 12.3 (2004), pp. 352–363. ISSN: 1063-6536. DOI: 10.1109/TCST.2004.824312.

[15] Lorenzo Serrao, Simona Onori, and Giorgio Rizzoni. "A Comparative Analysis of Energy Management Strategies for Hybrid Electric Vehicles". In: *Journal of Dynamic Systems, Measurement, and Control* 133 (2011).

[16] Wassif Shabbir. *Control Strategies for Series Hybrid Electric Vehicles*. PhD Thesis, 2015.

[17] Wassif Shabbir and Simos A. Evangelou. "Exclusive Operation Strategy for the Supervisory Control of Series Hybrid Electric Vehicles". In: *IEEE Transactions On Control Systems Technology* 24.6 (2016), pp. 2190–2198.

[18] Yu Wang and Zongxuan Sun. "Dynamic Analysis and Multivariable Transient Control of the Power-Split Hybrid Powertrain". In: *IEEE Transactions on Mechatronics* 20.6 (2015), pp. 3085–3097.

[19] Xingda Yan et al. "Portable Automobile Data Acquisition Module (ADAM) for Naturalistic Driving Study". In: *15th EAEC European Automotive Congress*. 2017.